Sub-Poissonian angular momentum distribution near threshold in atomic ionization by short laser pulses

Diego G. Arbó,[1,2] Konstantinos I. Dimitriou,[3,4] Emil Persson,[1] and Joachim Burgdörfer[1]
[1]*Institute for Theoretical Physics, Vienna University of Technology, Wiedner Hauptstraße 8-10/136, A-1040 Vienna, Austria, EU*
[2]*Institute for Astronomy and Space Physics, IAFE, CC 67, Suc. 28 (1428) Buenos Aires, Argentina*
[3]*Physics Department, Faculty of Applied Mathematics and Physics, National Technical University, Athens, Greece, EU*
[4]*Theoretical and Physical Chemistry Institute, National Hellenic Research Foundation, Athens, Greece, EU*
(Received 7 April 2008; published 9 July 2008)

We analyze the angular momentum distribution of electrons near threshold in atomic ionization by short laser pulses. The radial fanlike pattern in the two-dimensional momentum distribution observed in experiments is controlled by the dominance of a few angular momenta of the order l_0. We find a semiclassical expression for l_0 strongly dependent on the quiver amplitude of the detached electron but independent of the atomic species. The value of l_0 can be also related to the minimum number of absorbed photons needed to reach the threshold. The strongly peaked sub-Poissonian angular distribution precludes a description by a stochastic random walk model in angular momentum.

DOI: 10.1103/PhysRevA.78.013406 PACS number(s): 32.80.Rm, 32.80.Fb, 03.65.Sq

I. INTRODUCTION

As increasingly shorter laser pulses (fs) have become available, the interaction of few-cycle pulses with matter has attracted considerable interest. Rudenko *et al.* [1] and Maharjan *et al.* [2] presented fully two-dimensional momentum maps in cylindrical coordinates (k_z,k_ρ) for laser-ionized electrons for different rare gases, displaying a complex pattern. While at high momenta remnants of above threshold ionization (ATI) peaks are visible, near threshold a radial pattern with a shape of a bouquet has been both experimentally observed and theoretically calculated [3–7]. The origin of near-threshold structures has only recently been semiclassically explained in terms of a classical angular momentum (L) distribution sharply peaked near the quantum number l_0 [4]. Such distribution in the near-threshold continuum results from the interplay between the laser and the Coulomb fields [5]. The role of the Coulomb potential on the momentum spectrum is reflected in the focusing effect [8] and the strong laser field also influences the tunneling rate [9]. If, in addition, a multitude of paths reaching all emission angles and having nearly the same angular momentum L near l_0 exists, an interference pattern in complete analogy to generalized Ramsauer-Townsend (GRT) diffraction oscillations in electron-atom (or ion) scattering develops [4]. Clearly, underlying this semiclassical argument is the assumption that l_0 is large and well defined only within the residual quantum uncertainty. Such an analysis implies that the appearance of the interference pattern is "universal" in the sense that it is largely independent of the atomic core potential. More recently, the relation between l_0 and the minimum number N of absorbed photons to reach the continuum was empirically found [6] and explained in terms of a biased random walk model.

In the present work we extend the study of ionization of hydrogen atoms by short laser pulses performed in Ref. [4] to rare gas atoms. We present results of momentum distribution of emitted electrons by solving the time dependent Schrödinger equation (TDSE) and analyze the near-threshold structures for different atomic species of the target. We also have performed classical-trajectory Monte Carlo calculations [10] incorporating the tunneling (CTMC-T) through the potential barrier stemming from both nonperturbative Coulomb and laser field interactions. We find, indeed, that the peaked angular momentum distribution and the resulting electron emission pattern are only weakly dependent on the atomic species. We confirm the empirical relation between l_0 and N and provide a microscopic and quantitative explanation in terms of the properties of interfering classical trajectories of electrons in the presence of both the Coulomb and the laser fields. Atomic units are used throughout.

II. METHOD

The Hamiltonian of an atom interacting with a linearly polarized laser field within the single electron approximation is

$$H = \frac{\vec{p}^2}{2} + V(r) + \vec{r}\cdot\vec{F}(t), \tag{1}$$

where $\vec{p}$ and $\vec{r}$ are the momentum and position of the electron, respectively, $V(r)$ is the atomic central potential, and $\vec{F}(t)$ is the time dependent external field. The laser pulse is chosen to be of the form

$$\vec{F}(t) = F_0 \cos^2\left(\frac{\pi t}{\tau}\right)\cos(\omega t + \varphi_{CE})\hat{z}; \quad -\tau/2 \leqslant t \leqslant \tau/2, \tag{2}$$

and zero elsewhere. In Eq. (2), ω is the laser carrier frequency, φ_{CE} is the carrier-envelope phase, τ is the total pulse duration, F_0 the peak field, and $\hat{z}$ is the polarization direction.

Different techniques to solve the time-dependent Schrödinger equation (TDSE) [9,11–16] have been employed. Approximation methods include semiclassical approaches [17–19], the (Coulomb-)Volkov approximation [5,20,21], and the CTMC-T method [10,22]. In order to nu-

merically solve the TDSE we employ the generalized pseudospectral method [23–25]. This method combines a discretization of the radial coordinate optimized for the Coulomb singularity with quadrature methods to allow stable long-time evolution using a split-operator method. Both the unbound as well as the bound parts of the wave function $|\psi(t)\rangle$ can be accurately represented. The calculation of the 2D momentum distribution requires projection of the wave function $|\psi(\tau/2)\rangle$ after the conclusion of the pulse onto outgoing continuum functions [11,26,27]

$$\frac{dP}{d\vec{k}} = \frac{1}{4\pi k}\left|\sum_l e^{i\delta_l(k)}\sqrt{2l+1}P_l(\cos\theta)\langle k,l|\psi(\tau/2)\rangle\right|^2. \quad (3)$$

In Eq. (3), $\delta_l(k)$ is the momentum-dependent atomic phase shift, θ is the angle between the electron momentum $\vec{k}$ and the polarization direction of the laser field $\hat{z}$. P_l is the Legendre polynomial of degree l, and the partial wave $|k,l\rangle$ is the eigenstate of the atomic Hamiltonian with positive eigenenergy $E=k^2/2$ and orbital quantum number l. The atom is initially in its ground state. Due to the cylindrical symmetry for a linearly polarized laser field, the projection of the angular momentum onto the polarization axis is a constant of motion (i.e., the magnetic quantum number $m=0$). The distortion of the momentum distribution due to long-range final-state Coulomb interactions is fully accounted for in Eq. (3).

In order to delineate the classical properties of the strong-field ionization, we also employ a classical trajectory Monte Carlo method including tunnel effects (CTMC-T) [10,22]. The CTMC-T method excludes, because of its classical nature, any true multiphoton absorption process. We choose the microcanonical ensemble [28] to represent the initial ground state restricting the projection of the angular momentum L to the quantization axis, i.e., $|L_z|\leqslant 0.5$. The distribution in L will be discussed in Sec. IV. We let the initial ensemble evolve in time in the presence of the laser pulse by numerically integrating the classical equations of motion. The electron is allowed to tunnel through the potential barrier whenever it reaches the outer turning point, where $p_z=0$ and $zF(t)<0$, with a tunneling probability given by the WKB approximation [29]. At that moment the electron trajectory bifurcates: It either tunnels through the potential barrier or continues inside the potential barrier (for details see [30]). The bifurcation procedure is repeated at each encounter with the outer turning point until the end of the pulse for a given set of initial conditions. We note that since the WKB formula is strictly valid only for one-dimensional systems, application to the 3D problem requires the choice of an appropriate tunneling path. We choose for the evaluation of tunneling probability the path across the barrier which maximizes the tunneling probability on the energy manifold. Hamilton's equations of motion must be integrated well beyond $t=\tau/2$ in order to properly account for Coulomb final-state interactions on a classical level. From the classical trajectory distributions, ionization probabilities as well as probability distributions for the angular momenta of the ejected electron are determined.

III. SEMICLASSICAL ESTIMATES

The range of dominant angular momenta l_0 can be determined semiclassically in the tunneling regime. According to the CTMC-T calculations, a typical electron trajectory after tunneling shows a quiver motion along the polarization of the laser field superimposed on a drift motion following a Kepler hyperbola with the same final momentum [4]. The Kepler trajectory corresponds to the electronic motion under the effect of the atomic potential in the absence of the external electric field. To be precise, the emitted electron follows a Kepler hyperbola only for the case of a pure Coulombic potential i.e., $V(r)=-Z_T/r$, where Z_T is the charge of the remaining ionic nucleus. The departure of rare gas atomic potentials from the pure Coulomb potential is confined to a small region near the nucleus (of about a few atomic units). For this reason, only small deviations from the Kepler trajectories can take place. If the classical angular momentum distribution dP/dL is sharply peaked near l_0, and small contributions in Eq. (3) are neglected, it can be easily seen that the corresponding quantum ionization probability is expected to be proportional to $dP/d\vec{k}\approx[P_{l_0}(\cos\theta)]^2$ giving rise to a fan-shaped emission pattern with l_0 nodal lines. When the angular momentum distribution is somewhat broader encompassing a band of l states with width Δl, this pattern will be distorted but still visible as long as Δl is considerably smaller than l_0. The latter follows from the semiclassical limit of the Legendre polynomials, $P_{l_0}(\cos\theta)\sim\cos(l_0\theta)$.

Semiclassically, the oscillatory pattern results from interfering trajectories released at different times (near different extrema of the laser field) reaching the same asymptotic branch of the Kepler hyperbola. The number of quiver oscillations along the Kepler orbit reaching the same asymptote is not unique, thus allowing for path interferences. As the angular momentum of the Kepler hyperbola is identical to that of the asymptotic angular momentum L of the laser-driven electron, we can identify the pericenter of the hyperbola [31] with the quiver amplitude, $\alpha=(\sqrt{Z_T^2+(kL)^2}-Z_T)/k^2$, with $\alpha=F_0/\omega^2$ and Z_T the asymptotic charge of the atomic potential. This identification results in a simple and fit-parameter free relation between the classical angular momentum L and quiver amplitude α,

$$L(k) = (2Z_T\alpha + \alpha^2k^2)^{1/2}. \quad (4)$$

When we consider electrons with zero final kinetic energy (at threshold), Eq. (4) reduces to

$$L_0 = L(0) = (2Z_T\alpha)^{1/2}. \quad (5)$$

Identifying the classical angular momentum with the orbital angular momentum quantum number, i.e., $L\simeq l+1/2$, the number of quantum interference minima in the angular distribution near threshold can be predicted. The simple classical formula [Eq. (5)] predicts a "universal" L_0 value irrespective of the atomic species provided that the long range Coulomb force dominates. Only the net charge Z_T and the quiver amplitude enters. Two limitations of Eqs. (4) and (5) should be emphasized: (i) the classical expression does not consider discrete parity selection rules that may favor even or odd l_0; and moreover, (ii) L_0 is a real number while l_0 is

restricted to integers. Therefore, Eq. (5) can be expected to be valid within the quantum "binning" of classical angular momenta $L_0 \pm 1$. In the semiclassical limit $L \approx l \gg 1$, discreteness becomes negligible.

Recently, an empirical relation between the dominant l_0 and the minimum number N of photons needed for ionization was established [6]. Such a description involves explicitly a multiphoton absorption picture. This model involves a discrete walk in angular momentum space. A similar random walk model for the production of high l states has been previously proposed for multiple charged-particle scattering in ion-solid collisions [32]. Underlying such a model is a Poissonian random process described by a Fokker-Planck equation. Accordingly, l_0 can be associated with either the peak value or, alternatively, the first moment of the resulting distribution function p_l after N photons have been absorbed.

It is now instructive to combine a multiphoton analysis with the semiclassical description of the angular momentum distribution. The only dependence of the dominant angular momentum at threshold on the minimum number of absorbed photons to reach the continuum, N, results from conservation of energy,

$$E_N - E_0 = N\omega - U_p, \tag{6}$$

where $U_p=(F_0/2\omega)^2$ is the ponderomotive energy, and E_0 is the energy of the initial atomic state (the ground state in our case). For electrons at threshold, the minimum energy transfer required for ionization vanishes, i.e., $E_N=0$, and, therefore, the following relation between ω, F_0, E_0, and N

$$0 = N\omega - \left(\frac{F_0}{2\omega}\right)^2 + E_0 \tag{7}$$

is obtained. The cubic equation in ω [Eq. (7)] has only one real root ω_0, which is given in terms of F_0, E_0, and N by

$$\omega_0(F_0,E_0,N) = \frac{1}{6N}\left(-2E_0 + \frac{4E_0^2}{A^{1/3}} + A^{1/3}\right) \tag{8a}$$

with

$$A = 27N^2F_0^2 + 8E_0^3 + 3\sqrt{3}NF_0\sqrt{27N^2F_0^2 + 16E_0^2}. \tag{8b}$$

Inserting Eq. (8a) into the quiver amplitude $\alpha = F_0/[\omega_0(F_0,E_0,N)]^2$, and the latter into the expression for the classically dominant angular momentum [Eq. (5)], we arrive in turn at

$$L_0(F_0,E_0,N) = \frac{(2Z_TF_0)^{1/2}}{\omega_0(F_0,E_0,N)}. \tag{9}$$

Equation (9) provides a fit-parameter–free analytical expression for the dominant angular momentum L_0 as a function of the minimum number of photons N needed to reach the continuum. In Eq. (9) the angular momentum L_0 depends, in addition to N, also on the laser field strength F_0 and the initial state energy E_0. Note that apart from E_0, the properties of the atomic species do not enter.

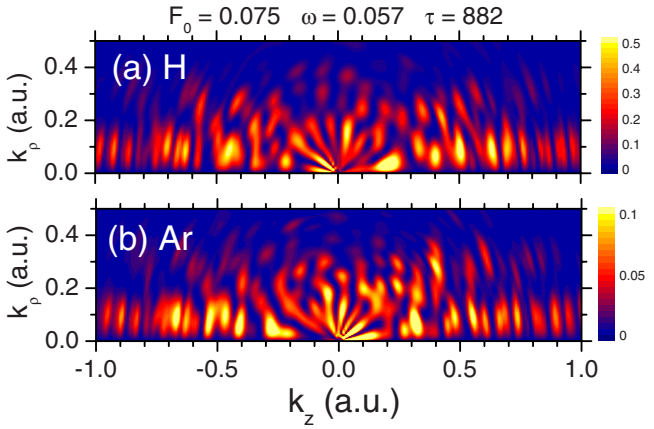

FIG. 1. (Color online) Doubly differential momentum distributions in cylindrical coordinates (k_z,k_ρ) of electrons in photodetachment from (a) H and (b) Ar. The parameters of the laser field are $\varphi_{CE}=0$, $\omega=0.057$, $F_0=0.075$, and $\tau=882$ (in a.u.).

IV. RESULTS

In Fig. 1 we show the two-dimensional momentum distribution, $\frac{d^2P}{dk_\rho dk_z}=2\pi k_\rho(\frac{dP}{dk})$, for photoionization of atomic hydrogen [Fig. 1(a)] and argon [Fig. 1(b)]. For the case of atomic argon, as we investigate single ionization processes, we reduce the multi-electron to a single active electron problem, i.e. only one electron is treated explicitly, while the rest of the electrons remain frozen. For this purpose we use a model potential in order to describe the interaction between the active electron with the rest of the ionic core. We chose the potential proposed by Muller [33] in Eq. (1) as it yields to the experimental binding energies of the ground and excited states of the Ar atom. The Keldysh parameter is defined as $\gamma=\sqrt{I_p/2U_p}$, where I_p is the ionization potential of the atom and $U_p=F_0^2/4\omega^2$ the ponderomotive energy. Resonant and nonresonant ionization has been thoroughly investigated from both the experimental and theoretical point of view for the case of Ar for infrared pulses in Ref. [16]. We consider in the following few cycle pulses, where Fourier broadening suppresses resonant excitation [34]. Note also that for the parameters of Fig. 1, the Keldysh parameter is low ($\gamma=0.76$ and 0.82 for hydrogen and argon) favoring nonresonant tunnel ionization. One point to be noticed in Fig. 1 is the similarity of the doubly differential momentum distributions for the two different atomic targets (hydrogen and argon). Both frames in Fig. 1 display complex interference patterns characterized by a transition from a ring-shaped pattern at larger $k=\sqrt{k_z^2+k_\rho^2}$ with circular nodal lines to a very different pattern of pronounced radial nodal lines for small k near threshold. The ring pattern is reminiscent of ATI peaks of the multiphoton regime ($\gamma>1$) and the bouquet-shaped radial nodal line develops inside the first ATI ring. The 2D momentum distributions in the transition regime ($\gamma\approx1$) exhibit evidences of both multiphoton transitions (at high k) and tunneling ionization (at low k).

In order to analyze the origin of the near-threshold pattern in more detail, we determine the distribution of contributing partial waves p_l within the first ATI ring, i.e., the partial

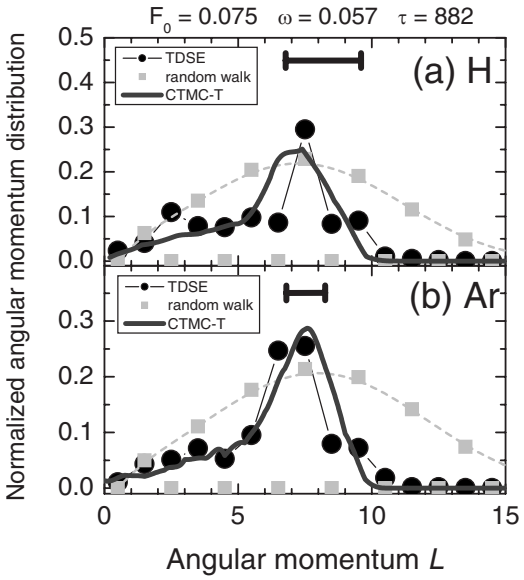

FIG. 2. Partial wave occupation probability p_l as a function of the angular momentum $L=l+1/2$ for the first ATI ring (see Fig. 2) for (a) H and (b) Ar. Dots correspond to TDSE calculations and gray squares to the random walk multiphoton model (connecting lines are only meant to guide the eye). The solid line shows the quasiclassical dP/dL distribution resulting from the CTMC-T calculation. The horizontal bar indicates the range of predicted values [Eq. (4)] for the dominant angular momentum L (see text). The parameters of the laser field are the same as Fig. 1.

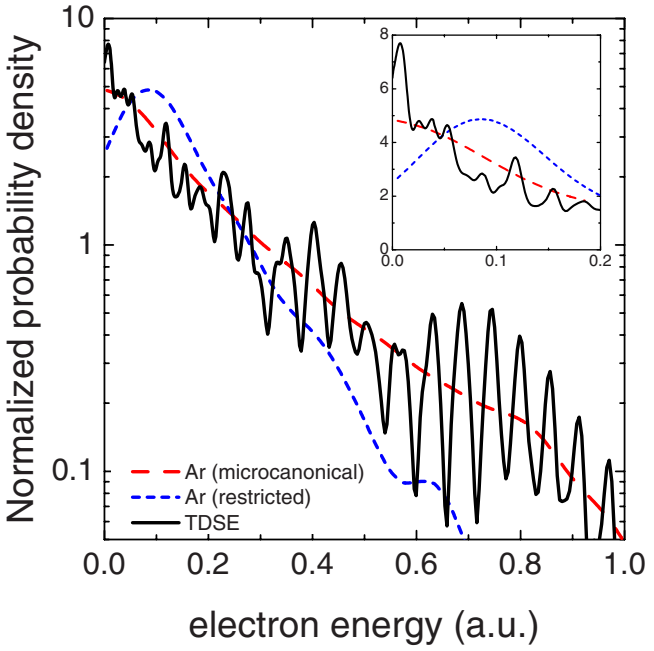

FIG. 3. (Color online) Photoelectron spectrum of Ar. (Black) thick solid line, TDSE; (red) thin dashed line, L-nonrestricted CTMC-T; and (blue) dotted line, restricted $(1<L<2)$ CTMC-T. The parameters of the laser field are the same as Fig. 1. The inset show the low energy features of the photoelectron spectrum in linear scaling.

ionization probability with orbital quantum number l up to the first minimum in the momentum Δ [4],

$$p_l = \int_0^{\Delta} k dk |\langle k,l|\psi(\tau)\rangle|^2. \tag{10}$$

The value of Δ can either be obtained graphically from the distribution of emitted electrons (Fig. 1) or numerically from the midpoint energy between first and second ATI in the continuum, i.e., $\Delta^2/2=(E_N+E_{N+1})/2$, where E_N is given by Eq. (6). In our case $\Delta \simeq 0.3$ and 0.2 for the case of hydrogen and argon, respectively.

In Fig. 2 we show the partial-wave distributions obtained from the TDSE calculations where we have used the prescription $L=l+1/2$. We can observe in Fig. 2 that the partial-wave distributions near threshold peak at $l_0=7$ for both hydrogen and argon cases. This is in excellent agreement to the prediction for $L=6.8$ from Eq. (4), which is the lower limit of the predicted L range shown in both Figs. 2(a) and 2(b). The upper limits of the range correspond to the value $L(\Delta)$ calculated through Eq. (4). The p_l distribution exhibits a quantitative similarity between the emission pattern for hydrogen and argon more clearly than the qualitative resemblance of the doubly differential momentum distribution. For the case of hydrogen the number of minima in the angular distribution [Fig. 1(a)] is equal to the value of the dominant angular momentum, i.e., $l_0=7$ $(L_0=7.5)$. In turn, for the case of argon [Fig. 1(b)] the angular distribution corresponds predominantly to the coherent sum of two Legendre polynomials of degree 6 and 7 resulting in a slight blurring of the nodal lines.

In order to highlight the underlying classical dynamics, we include in Fig. 2 results of the CTMC-T calculations for both hydrogen and argon. The continuous quasiclassical angular momentum distribution dP/dL reproduces the discrete TDSE p_l distributions very well for hydrogen and argon within the limits of quantum discreteness. We employ for both hydrogen and argon the same initial microcanonical ensemble with L unrestricted. The latter is not unambiguous for Ar (ground state configuration $2p^6$). We have verified that the unrestricted ensemble reproduces, apart from discrete multiphoton peaks, the quantum photoelectron spectrum remarkably well (Fig. 3). A simulation restricting L to $1 \leqslant L \leqslant 2$ shows poor agreement with the quantum spectra and provides independent support for the unrestricted microcanonical ensemble. Not only the position of the maximum in p_l but also the narrow width of the distribution is accounted for by the CTMC-T (Fig. 2). This is an indication that in this regime the atomic ionization is dominated by a tunneling process, in line with a Keldysh parameter smaller than one for both hydrogen and argon cases.

The width of the l-distribution can also be used to test the random walk model for the angular momentum distribution. The peak (or most probable) value l_0 $(\geqslant 1)$ is in this context viewed as the result of a sequence of a large number of randomly angular momentum changing photoabsorption processes [6] assuming a stochastic uncorrelated multiphoton process. In the present case of multiphoton absorption, one electron with orbital quantum number l can absorb a photon and consequently undergoes a transition $l \rightarrow l+1$ with a prob-

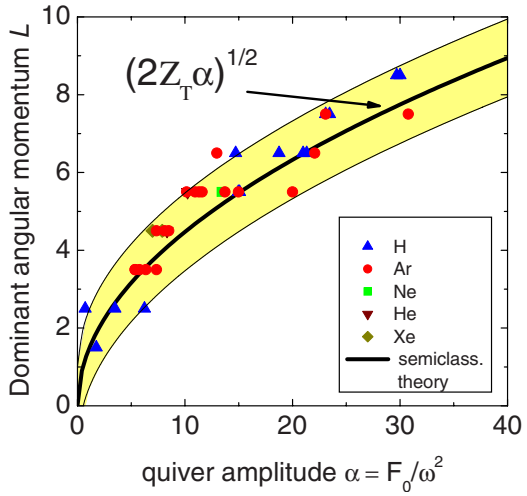

FIG. 4. (Color online) Dominant angular momentum $L_0=l_0+1/2$ as a function of the quiver amplitude α. Dots, different *ab initio* TDSE calculations for H, Ar, Ne, He, and Xe [3,4,6,7,11,16]. Thick solid line: semiclassical prediction [Eq. (4)]. Shaded area corresponds to the uncertainty of the semiclassical prediction due to the quantum discreteness (see text).

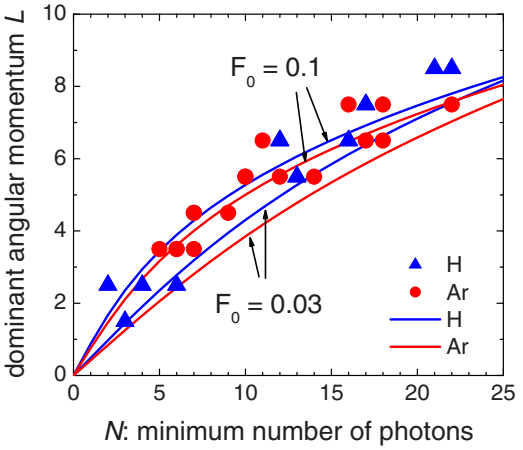

FIG. 5. (Color online) Dominant angular momentum L_0 as a function of the minimum number N of photons needed to ionize H and Ar atoms. Different *ab initio* TDSE calculations for H (blue triangles) and Ar (red dots). Solid line, semiclassical prediction [Eq. (9)] for two different peak fields, $F_0=0.03$ and 0.1 for H (blue) and Ar (red). In all TDSE calculations $0.03<F_0<0.1$.

ability p_+ or a transition $l\rightarrow l-1$ with a probability p_-, according to the dipole coupling. It is well known that single photonabsorption leads to a preference of populating higher angular momentum states in excitation processes. This corresponds to a biased random walk. A total number of $N=17$ and 18 photons is needed to reach the continuum for the cases of Fig. 2(a) in hydrogen and Fig. 2(b) in argon, respectively. Therefore, according to the selection rule $\Delta l=\pm 1$, and considering that the ground state for hydrogen is an s state and for argon a p state, only odd partial waves are populated, as shown in Figs. 2(a) and 2(b). For the first moment, reasonable agreement with the TDSE result can be found by choosing suitable values for p_+ and p_-. Indeed, choosing $p_+=2/3$ and $p_-=1/3$ the peak position l_0 can be well reproduced (Fig. 2). However, in a Poissonian random walk process, the first and second moments, or equivalently, the peak position l_0 and the width σ of the angular momentum distribution are interrelated and both are proportional to N (the number of steps of the random walk). Consequently, we find a broad p_l distribution (Fig. 2) at variance with both the TDSE and the quasiclassical CTMC-T results. The latter clearly shows the sub-Poissonian nature of the interaction process proper of the tunneling regime for Keldysh parameters near unity.

In Fig. 4 we plot the dominant angular momenta $L_0=l_0+1/2$ of different exact TDSE calculations [3,4,6,7,11,16] as a function of the quiver amplitude α for different atomic species (H, Ar, Ne, He, and Xe) and compare them to our semiclassical prediction for L [Eq. (4)] where we include also the uncertainty of the classical description due to the quantum discreteness ($L\pm 1$) discussed above as the shaded area. Very good agreement is observed. The similarity of the dominant angular momenta for the different atomic species confirms the minor influence of the details of the core potential on the emission distribution. Only the asymptotic charge Z_T is relevant since after tunneling the continuum electron propagates at large distances from the nucleus where the combined laser and asymptotic Coulomb fields determine the trajectory. Note that in the energy regime considered rescattering is not important.

The dependence of the dominant angular momentum on the minimum number of photons to reach the continuum for two different values of the peak electric field, i.e., $F_0=0.03$ and 0.1 [Eq. (9)] is displayed in Fig. 5 for both hydrogen and argon. We compare to results of the TDSE calculations of Fig. 4 for hydrogen and argon, which were performed for laser fields between the values: $F_0=0.03$ and 0.1. The agreement is, overall, very good. Note, however, that such a semiclassical estimate is expected to break down when only few (of order unity) photons are needed for ionization.

V. CONCLUSIONS

In conclusion, for photoionization of atoms by few-cycle laser pulses, we have shown that doubly differential momentum distributions near threshold exhibit a radial nodal structure that results from peaked partial wave distribution p_l near a particular angular momentum l_0. We prove that for the Keldysh parameters used here ($\gamma\sim 1$) the narrow angular momentum distribution near threshold is the result of a tunneling process at variance with a broad Poissonian distribution resulting from a Poissonian random walk model. The narrow angular distribution is governed by predominantly one (or very few) partial waves, $dP/d\cos\theta\sim[P_{l_0}(\cos\theta)]^2$. This relation is reminiscent of generalized Ramsauer-Townsend diffraction oscillations [35]. As in the case of electron-ion scattering theory, it results from the existence of interfering paths under the influence of two competing forces, which are in the present case the atomic Coulomb potential and the electric field of the laser. We find that the dominant angular momentum near threshold depends strongly on the laser frequency and peak field but not on the atomic species. Within a semiclassical description we have

derived an analytic expression for the dominant angular momentum of slow electrons, which depends only on the quiver amplitude, or equivalently, on the ionization potential, the laser field amplitude, and the number of photons required for ionization and is largely independent of the atomic species of the target. This universal expression predicts the dominant angular momentum L_0 in excellent agreement with TDSE calculations for a variety of atomic targets.

ACKNOWLEDGMENTS

The authors thank G. F. Gribakin for suggesting the investigation of the random walk model. This work was performed with financial support of CONICET and ANPCYT PICT 772 of Argentina, by the SFB 016 ADLIS, Project No. P15025-N08 of the FWF (Austria), and by EU Projects No. HPRI-2001-50036 and No. HPRI-CT-2005-026015.

[1] A. Rudenko, K. Zrost, C. D. Schröter, V. L. B. de Jesus, B. Feuerstein, R. Moshammer, and J. Ullrich, J. Phys. B **37**, L407 (2004).
[2] C. M. Maharjan, A. S. Alnaser, I. Litvinyuk, P. Ranitovic, and C. L. Cocke, J. Phys. B **39**, 1955 (2006).
[3] A. de Bohan, Ph.D. thesis, Université Catholique de Louvain, 2001 (unpublished).
[4] D. G. Arbó, S. Yoshida, E. Persson, K. I. Dimitriou, and J. Burgdörfer, Phys. Rev. Lett. **96**, 143003 (2006).
[5] D. G. Arbó, J. E. Miraglia, M. S. Gravielle, K. Schiessl, E. Persson, and J. Burgdörfer, Phys. Rev. A **77**, 013401 (2008).
[6] Z. Chen, T. Morishita, A.-T. Le, M. Wickenhauser, X. M. Tong, and C. D. Lin, Phys. Rev. A **74**, 053405 (2006).
[7] M. Wickenhauser, X. M. Tong, D. G. Arbó, J. Burgdörfer, and C. D. Lin, Phys. Rev. A **74**, 041402(R) (2006).
[8] A. de Bohan, B. Piraux, L. Ponce, R. Taïeb, V. Véniard, and A. Maquet, Phys. Rev. Lett. **89**, 113002 (2002).
[9] D. Bauer and P. Mulser, Phys. Rev. A **59**, 569 (1999).
[10] K. I. Dimitriou, D. G. Arbó, S. Yoshida, E. Persson, and J. Burgdörfer, Phys. Rev. A **70**, 061401(R) (2004).
[11] S. Dionissopoulou, Th. Mercouris, A. Lyras, and C. A. Nicolaides, Phys. Rev. A **55**, 4397 (1997).
[12] Joseph Wassaf, Valérie Véniard, Richard Taieb, and Alfred Maquet, Phys. Rev. A **67**, 053405 (2003).
[13] E. Cormier and P. Lambropoulos, J. Phys. B **29**, 1667 (1996).
[14] E. Cormier and P. Lambropoulos, J. Phys. B **30**, 77 (1997).
[15] H. Bachau, E. Cormier, P. Decleva, J. E. Hansen, and F. Martín, Rep. Prog. Phys. **64**, 1815 (2001).
[16] R. Wiehle, B. Witzel, H. Helm, and E. Cormier, Phys. Rev. A **67**, 063405 (2003); E. Cormier, P.-A. Hervieux, R. Wiehle, B. Witzel, and H. Helm, Eur. Phys. J. D **26**, 83 (2003).
[17] G. F. Gribakin and M. Yu. Kuchiev, Phys. Rev. A **55**, 3760 (1997).
[18] Gerd van de Sand and Jan M. Rost, Phys. Rev. A **62**, 053403 (2000).
[19] D. B. Milosevic, G. G. Paulus, and W. Becker, Opt. Express **11**, 1418 (2003).
[20] P. A. Macri, J. E. Miraglia, and M. S. Gravielle, J. Opt. Soc. Am. B **20**, 1801 (2003).
[21] V. D. Rodriguez, E. Cormier, and R. Gayet, Phys. Rev. A **69**, 053402 (2004).
[22] J. S. Cohen, Phys. Rev. A **64**, 043412 (2001); **68**, 033409 (2003).
[23] X.-M. Tong and S. I. Chu, Chem. Phys. **217**, 119 (1997).
[24] X.-M. Tong and Shih-I Chu, Phys. Rev. A **61**, 031401(R) (2000).
[25] X.-M. Tong and C. D. Lin, J. Phys. B **38**, 2593 (2005).
[26] O. Schöller, J. S. Briggs, and R. M. Dreizler, J. Phys. B **19**, 2505 (1986).
[27] A. Messiah, *Quantum Mechanics 1* (North-Holland, New York, 1965).
[28] R. Abrines and I. C. Percival, Proc. Phys. Soc. London **88**, 861 (1966).
[29] E. C. Kemble, Phys. Rev. **48**, 549 (1935); M. S. Child, Mol. Phys. **12**, 401 (1967); J. N. L. Connor, *ibid.* **15**, 37 (1968).
[30] K. I. Dimitriou, S. Yoshida, J. Burgdörfer, H. Shimada, H. Oyama, and Y. Yamazaki, Phys. Rev. A **75**, 013418 (2007).
[31] L. D. Landau and E. M. Lifshitz, *Mechanics* (Pergamon, Oxford, 1960).
[32] J. Burgdörfer and C. Bottcher, Phys. Rev. Lett. **61**, 2917 (1988); J. Burgdörfer, in *Collisionally Induced Stochastic Dynamics of Fast Ions in Solids*, AIP Conf. Proc. No. 205 (AIP, New York, 1989), p. 476.
[33] H. G. Muller and F. C. Kooiman, Phys. Rev. Lett. **81**, 1207 (1998).
[34] F. Grasbon, G. G. Paulus, H. Walther, P. Villoresi, G. Sansone, S. Stagira, M. Nisoli, and S. De Silvestri, Phys. Rev. Lett. **91**, 173003 (2003).
[35] J. Burgdörfer, C. Reinhold, J. Sternberg, and J. Wang, Phys. Rev. A **51**, 1248 (1995).